

## Article

# Design, Implementation and Simulation of a Small-Scale Biorefinery Model

Mihaela Sbarciog <sup>†</sup> , Viviane De Buck , Simen Akkermans , Satyajeet Bhonsale , Monika Polanska   
and Jan F. M. Van Impe <sup>\*</sup> 

BioTeC+, Chemical and Biochemical Process Technology and Control, Department of Chemical Engineering, KU Leuven, 9000 Gent, Belgium; mihaelaiuliana.sbarciog@kuleuven.be (M.S.); viviane.debuck@kuleuven.be (V.D.B.); simen.akkermans@kuleuven.be (S.A.); satyajeetsheetal.bhonsale@kuleuven.be (S.B.); monika.polanska@kuleuven.be (M.P.)

<sup>\*</sup> Correspondence: jan.vanimpe@kuleuven.be

<sup>†</sup> Current address: 3BIO-BioControl, Université Libre de Bruxelles, 1050 Brussels, Belgium.

**Abstract:** Second-generation biomass is an underexploited resource, which can lead to valuable products in a circular economy. Available locally as food waste, gardening and pruning waste or agricultural waste, second-generation biomass can be processed into high-valued products through a flexi-feed small-scale biorefinery. The flexi-feed and the use of local biomass ensure the continuous availability of feedstock at low logistic costs. However, the viability and sustainability of the biorefinery must be ensured by the design and optimal operation. While the design depends on the available feedstock and the desired products, the optimisation requires the availability of a mathematical model of the biorefinery. This paper details the design and modelling of a small-scale biorefinery in view of its optimisation at a later stage. The proposed biorefinery comprises the following processes: steam refining, anaerobic digestion, ammonia stripping and composting. The models' integration and the overall biorefinery operation are emphasised. The simulation results assess the potential of the real biowaste collected in a commune in Flanders (Belgium) to produce oligosaccharides, lignin, fibres, biogas, fertiliser and compost. This represents a baseline scenario, which can be subsequently employed in the evaluation of optimised solutions. The outlined approach leads to better feedstocks utilisation and product diversification, raising awareness on the impact and importance of small-scale biorefineries at a commune level.

**Keywords:** biomass; biorefinery design; process integration; scheduling; simulation



**Citation:** Sbarciog, M.; De Buck, V.; Akkermans, S.; Bhonsale, S.; Polanska, M.; Van Impe, J.F.M. Design, Implementation and Simulation of a Small-Scale Biorefinery Model. *Processes* **2022**, *10*, 829. <https://doi.org/10.3390/pr10050829>

Academic Editors: Philippe Bogaerts and Alain Vande Wouwer

Received: 31 January 2022

Accepted: 15 April 2022

Published: 22 April 2022

**Publisher's Note:** MDPI stays neutral with regard to jurisdictional claims in published maps and institutional affiliations.



**Copyright:** © 2022 by the authors. Licensee MDPI, Basel, Switzerland. This article is an open access article distributed under the terms and conditions of the Creative Commons Attribution (CC BY) license (<https://creativecommons.org/licenses/by/4.0/>).

## 1. Introduction

Lignocellulosic biomass represents an abundant and sustainable carbon-rich feedstock that can be employed to produce, e.g., (bio-)chemicals, biofuels, fibres and nutrients. As the urge to employ sustainable processing methods and feedstocks is becoming ever greater with regard to climate change, interest in how to optimally process this feedstock has steadily increased over the past decade. To obtain valuable and useful products, the dense crystalline structure of lignocellulosic biomass needs to be broken down. The three main building-blocks of lignocellulosic biomass are: (i) lignin, (ii) cellulose and (iii) hemicellulose (see Figure 1). While cellulose is an extremely dense structure, mainly consisting of  $\beta(1 \rightarrow 4)$ -D-Glucose units, structured in a helical strand, hemicellulose and lignin are more diverse, containing a multitude of different compounds, the most important of which are represented in Figure 1.

The breakdown and conversion of lignocellulosic biomass in useful and value-added products occurs in a biorefinery. In [1], the authors presented a classification system to categorise biorefineries based on: (i) which platforms or intermediate products they used, (ii) the products they produced, (iii) the used feedstocks and (iv) the used processes. So-called first-generation biorefineries used food products, such as corn and wheat, as feedstock and

converted these starch-rich and uniform feedstocks into bulk products such as biofuels and other platform chemicals. In essence, these biorefineries were the biomass-based counterpart of regular petroleum refineries (where raw fossil oil is refined into value-added products). However, as they used food as feedstock and they competed with the food industry for arable land, these enterprises were faced with heavy criticism [1,2].

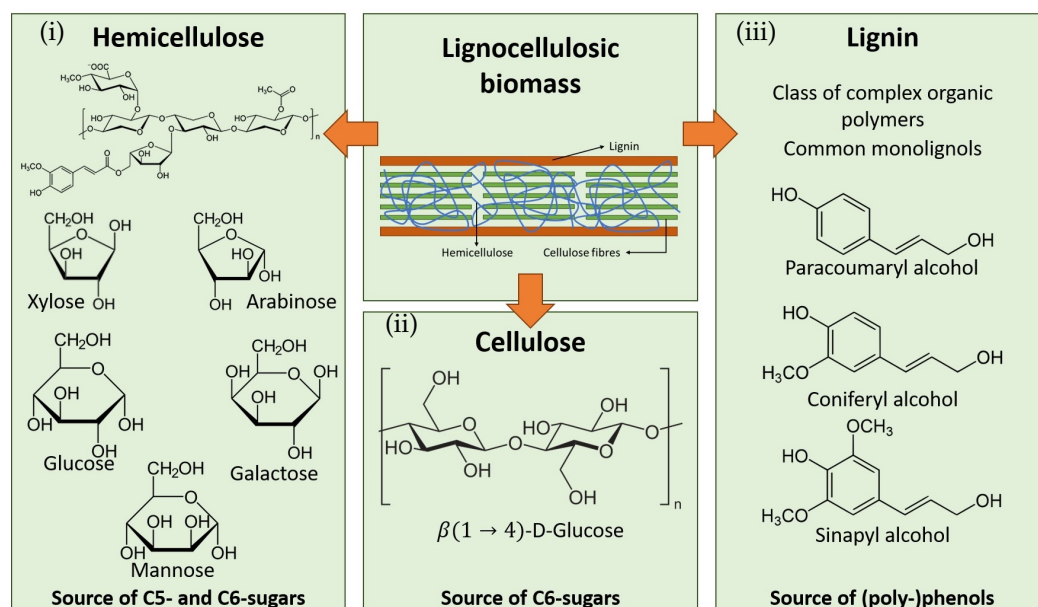


**Figure 1.** Schematic representation of lignocellulosic biomass and its three main building-blocks: (i) hemicellulose, (ii) cellulose and (iii) lignin (taken from [3]).

Second-generation biorefineries were developed as a response to this major flaw of first-generation biorefineries. In a second-generation biorefinery, the feedstock that is processed is a waste, or a non-food stream [1,2,4]. In particular, the usage of biowaste has become of great interest lately, as biowaste biorefineries additionally act as waste processing facilities [5], thus playing a central role in the circular economy. When regarding the application potential of biorefineries on a local level, their ability to revalorise biowaste in locally desired products is a compelling advantage [6,7]. (Lignocellulosic) Waste streams, however, have the major disadvantage that their composition, due to their waste nature, is no longer uniform [8,9]. Moreover, when only considering local biowaste streams, their periodic yields are also limited. Combined, these two disadvantages make biowaste streams unsuitable for the production of bulk products such as biofuels. Unlike first-generation biorefineries, the processes employed in a local and small-scale biorefinery need to be more robust and flexible, as the feedstock's composition may be variable. Additionally, the selected processes should render high-value products, as the overall feedstock throughput of the biorefinery will be limited due to its local nature [10]. In addition, Refs. [4,9] indicated that the production of fuels by biorefineries is inherently unsustainable. The combination of both considerations has led to a steady increase in interest regarding the production of high-value-added products from biowaste streams using biorefinery systems.

Even though the advantages of small-scale biorefineries have been indicated by multiple research studies, their implementation is lagging behind [6,7]. In particular, with regards to planning and designing a suitable small-scale and locally adapted biorefinery, decision-makers and investors are faced with a multitude of challenges and uncertainties. These uncertainties can often lead to the absence of the required investments to build biorefinery facilities. This, on its turn, leads again to an increased lack of trust in the considered systems [11,12]. (Online) Decision support tools (DST) are a convenient alternative for aiding decision-makers in designing the most suitable biorefinery systems for their particular settings as well as to increase their confidence in the proposed process layout [11,12].

An important part of developing a small-scale and locally embedded biorefinery consists of selecting the most suitable processes for converting locally available biowaste streams into value-added and desirable products [3]. Mathematical models of the considered processes allow for an easy assessment of the performance of the investigated processing chain. Moreover, mathematical models can be used to optimise the process flow-sheet itself as well as the processing conditions. Mathematical models of biorefinery conversion processes can range from static to dynamic models. Whereas the first type of models consider a steady-state process, i.e., time has no influence on the states of the process, a dynamic model allows for a more accurate prediction of the process's states and outputs, which are inherently influenced by the time variation of the inputs and disturbances acting on the process. Especially when considering batch processes, such as steam refining and composting, the duration of the process has a major influence on the process outcome. An additional advantage of dynamic models is that they allow for optimising the way a biorefinery is operated, i.e., imposing an (on-line) optimal control system on the biorefinery [13,14]. Static process models would only allow for a yield-based process optimisation. With regard to optimising the process flow-sheet itself, often, the so-called superstructure modelling system is employed [15–17]. To increase the extendability and user-friendliness of these superstructure models (which often consider a vast amount of different processes and/or process combinations), a simplified and generalised modelling framework is employed for all the considered processes. In this contribution, a similar superstructure model is being developed; however, as the scope of the foreseen biorefinery is limited to local and small-scale processing of biowaste streams, the number of processes selected using expert knowledge is limited. Moreover, as the eventual goal is to submit the proposed design to a process and a control optimisation, dynamic models have been selected for the considered processes. The developed model can be used in the first stage to assess the potential of locally available biowaste for producing value-added products. Subsequently, it may be employed to optimise the entire operation of the biorefinery in view of maximising the production of desired products. The model can be integrated together with a bioinventory tool, which provides a survey of the available biowaste, and an optimisation tool, which may take into account also sustainable indicators, into a decision support tool that allows for the design of small-scale, flexi-feed, sustainable biorefineries in a local setting.

The remainder of this contribution consists of a thorough discussion on the design of a local small-scale biorefinery in Section 2, followed by an in-depth discussion in Section 3 on the employed models for each process that was incorporated in the design, the models' integration and the biorefinery operation. Section 4 focuses on the obtained results from simulating the biorefinery operation for the biowaste available in a commune in the Flanders region. Finally, conclusions, as well as some remarks with regard to future research, are drawn in Section 5.

## 2. Biorefinery Design

A biorefinery can be simply considered to consist of three parts that are linked together: (i) the input or feedstock part, (ii) the process part and (iii) the output or product part. All three parts come with their own set of distinct (strategical) design choices that need to be considered when designing a biorefinery system (see Figure 2) [18]. Moreover, the choices made in one part of the biorefinery system will inevitably influence the choices that have to be made with regard to the other parts. To illustrate this, when the biorefinery is designed with the ethos of producing a certain product, e.g., biofuel, only a small set of suitable conversion processes and feedstocks will remain eligible for selection.

A local and small-scale biorefinery should tailor for local needs: local feedstocks should be converted into locally desired products. As the biorefinery system proposed in this contribution should additionally function as a waste-processing facility, the overall biorefinery system is designed starting from the feedstock part.

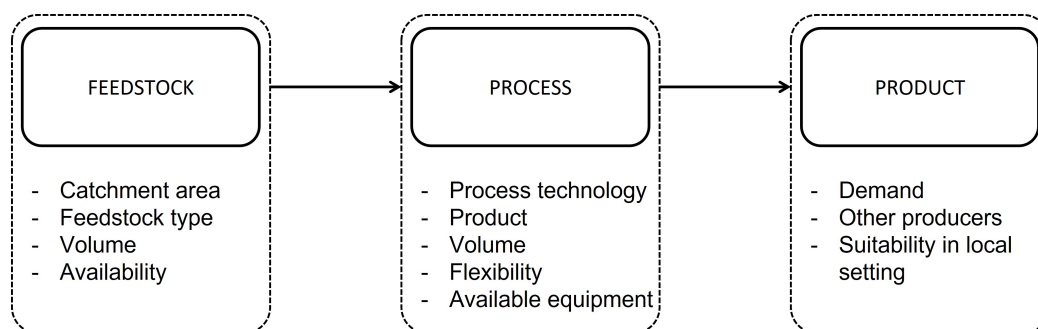


**Figure 2.** Simplified outline of a biorefinery with its three parts (feedstock, process and product), and their respective main strategic decisions (taken from [18]).

When designing a biorefinery from the feedstock side, one of the main aspects to consider is which feedstock is supposed to be processed by the facility. The most optimal conversion processes for a dense and highly crystalline feedstock will differ considerably from those employed when a soft feedstock is being processed. Additionally, the selection of certain conversion processes over others will have an influence on which volumes the biorefinery can handle and/or which products the facility will render.

### 2.1. Designing a Local Small-Scale Biorefinery

The two main lignocellulosic feedstocks that should be considered in a Flemish setting are kitchen waste and wood waste obtained from garden and landscape maintenance. Based on expert knowledge, a set of flexible and robust processes which are able to process either one or both of the considered feedstock streams were selected. The concatenation of the proposed conversion processes was obtained by employing a reverse-engineering design approach. More specifically, for each of the proposed feedstocks and for all of the proposed conversion processes, which products could be obtained was assessed. Based on the selected (set of) products, the required processes were coupled in such a way that the net flow of waste streams, i.e., undervalorised outflows of organic material, was minimised.

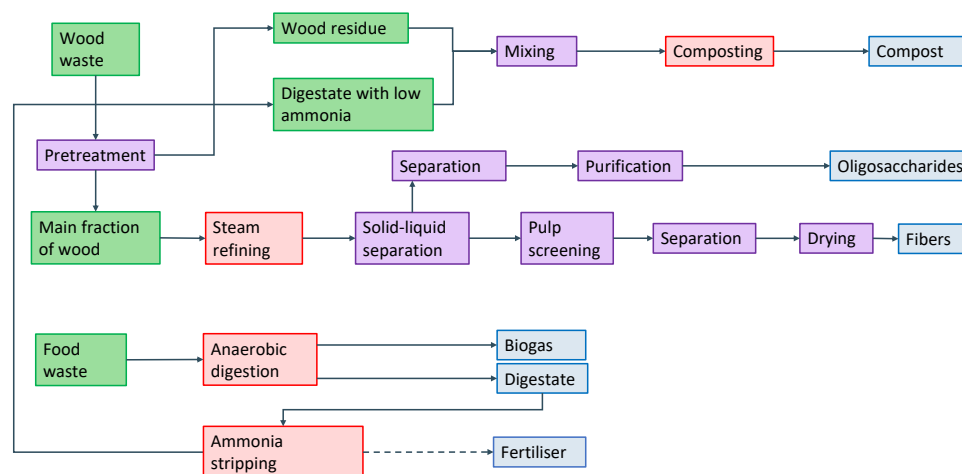
### 2.2. Proposed Integrated Small-Scale Biorefinery for a Flemish Setting

Figure 3 displays the eventually obtained flow-sheet of the small-scale biorefinery that will be presented and modelled in this contribution. Note that this flow-sheet represents the overarching, or superstructure, of the proposed small-scale and flexi-feed biorefinery in a Flemish setting. Depending on which products the biorefinery operators are interested in and/or their local circumstances with regard to equipment, the flow-sheet can be adapted to fit these local needs.

The main processes have been selected based on the foreseen feedstocks that could be processed by the biorefinery, i.e., two major lignocellulosic feedstocks that can be found in the case study region of Flanders: kitchen waste and (postconsumer) wood waste. Four main processes have been selected based on expert knowledge: (i) steam refining, (ii) anaerobic digestion, (iii) ammonia stripping and (iv) composting.

The four main processes are concatenated in such a way that the waste/output streams of each process are, on their turn, maximally utilised. This overarching integrated biorefinery design has been defined using expert knowledge.

Wood waste obtained from garden and landscape maintenance (i.e., pruning waste) is initially submitted to a pretreatment step consisting of chipping and sieving. Small enough wood chips are processed using steam refining, whereas bigger pieces (on average, this residue stream accounts for 5% of the total wood waste) are processed directly via a composting process.



**Figure 3.** Schematic representation of the small-scale biorefinery modelled in this contribution. (Intermediate) Feedstocks are represented in green, main processes are represented in red, secondary processes are represented in purple, and (intermediate) products are represented in blue.

A steam refiner is, in essence, a mill consisting of two grinding wheels spinning in opposite directions between which the wood chips are ground down. To facilitate this process, steam is injected in the mill to weaken the crystalline structure of the lignocellulosic chips and to extract small molecules from the wood chips. The two main product categories of a steam refining process are solid fibres and a liquid extract containing a broad range of components, e.g., oligosaccharides. The obtained fibres can be further processed into paper, while the extract stream can be further refined to nutrients, tensides, etc.

Kitchen waste is a fairly soft feedstock and therefore does not require severe conversion processes like wood waste does. In the region of Flanders, kitchen waste that is collected via home-to-home collection rounds is of compostable quality. However, when aiming to maximise the potential of this particular feedstock, other conversion processes can take place prior to the final composting step. As kitchen waste is a nitrogen-rich feedstock, it lends itself perfectly to being processed using an anaerobic digestion step, followed by an ammonia stripping step.

An anaerobic digester is a continuous process during which the input stream is broken down, in the absence of oxygen, by bacteria into biogas and digestate. Biogas is a mix of methane ( $CH_4$ ), carbon dioxide ( $CO_2$ ) and hydrogen ( $H_2$ ), whereas digestate is a nitrogen-rich waste stream. Anaerobic digestion is one of the most commonly applied biorefinery processes. In particular, countries such as Germany and France are at the forefront with regard to biomethane facilities, with 232 and 131 biomethane plants, respectively [19]. The quality of the produced biogas is defined by the amount of  $CH_4$  in the output stream, i.e., the more methane, the higher the quality of the biogas. The methane percentage in biogas can be optimised by either adjusting the process parameters (see also Section 3.2) or adjusting the composition of the feedstock streams that are entering the biorefinery. The latter can, for instance, be artificially obtained by mixing two feedstocks together [20].

Even though anaerobic digestion is a flexible process, which has been employed for the conversion of manure, wastewater sludge and other recalcitrant organic waste streams [21], it has the disadvantage that the conversion process is coupled with the production of a steady and nitrogen-rich waste stream: the digestate. As nitrogen is not dissimilated during the digestion process, it accumulates in the digester's nongaseous output stream. In the case study region of Belgium, processing such high volumes of a nitrogen-rich waste stream cannot be accomplished without removing the bulk of the nitrogen content from the waste stream. Moreover, the nitrogen still present in the digestate stream can be used to produce a nitrogen fertiliser. Unbound nitrogen (i.e., in its  $NH_3/NH_4^+$  state) can be easily removed from a liquid stream at increased pH using air stripping.

The remaining digestate stream, now with low nitrogen content, still represents a constant and relatively high flow of organic material that can still be further processed. The final step in the proposed biorefinery design consists of a composting step of the digestate combined with the residual wood waste that could not be processed using the steam refining process. Whereas the anaerobic digestion and ammonia stripping are operated in a continuous mode, the composting process is operated as a batch process. Switching from a continuous production line to a batch-operated production line requires a decoupling, often obtained by the usage of holding tanks. Holding tanks can store the continuously produced input of the batch process until the batch reactor is available again. This topic is detailed in the next section.

### 3. Materials and Methods

#### 3.1. Steam Refining

The steam refining model used in this biorefinery setup is a kinetic model developed in [22,23] for the treatment of birch wood at temperatures in the range  $[180, 240]^\circ\text{C}$ , with the concept of a wood biorefinery in view. This implies the selective separation of the three main wood components (lignin, cellulose/xylose and hemicellulose/glucan), which may be further used for the production of high-value components. Consequently, the model includes the three main processes, i.e., delignification, degradation and conversion of xylan and degradation and conversion of glucan, which are briefly described below. The efficiency of the treatment is determined by the experiment temperature and duration. A schematic representation of the steam refining process is illustrated in Figure 4.

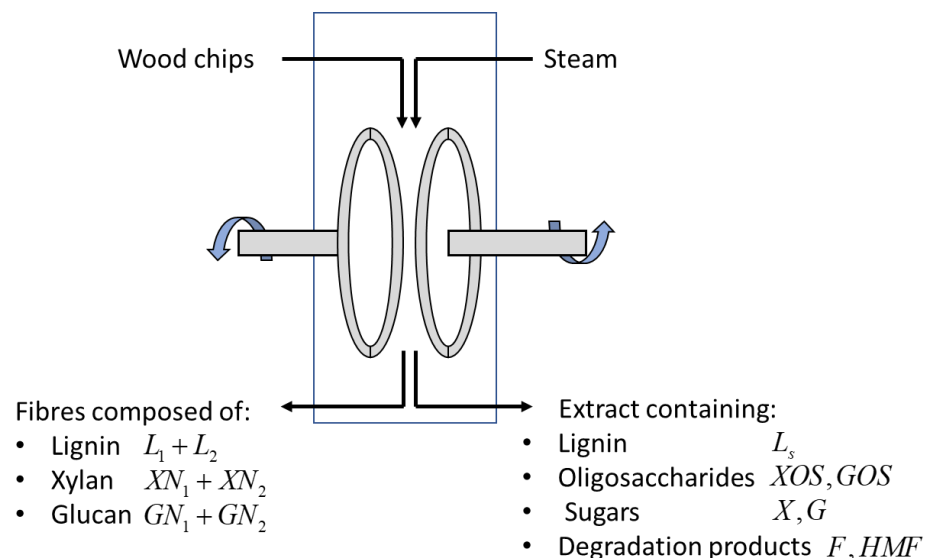


**Figure 4.** Schematic representation of a steam refiner.

The delignification process consists of a solubilisation reaction and a condensation reaction. In the solubilisation reaction, the lignin in the solid, which is divided into a hard-to-remove fraction  $L_1$  and an easy-to-remove fraction  $L_2$ , is converted into solubilised lignin  $L_s$ . In the condensation reaction, a part of the solubilised lignin returns to the solid phase as condensed lignin  $L_c$ . Hence, the amount of lignin in the solid phase is determined by the sum  $L_1 + L_2 + L_c$ , while the amount of lignin in the extract is determined by  $L_s$ . The delignification process is mathematically described by:

$$\begin{aligned}
 \frac{dL_1}{dt} &= -k_{s1}L_1 \\
 \frac{dL_2}{dt} &= -k_{s2}L_2 \\
 \frac{dL_s}{dt} &= k_{s1}L_1 + k_{s2}L_2 - k_cL_s \\
 \frac{dL_c}{dt} &= k_cL_s
 \end{aligned}
 \tag{1}$$

where  $k_{s1}$ ,  $k_{s2}$  and  $k_c$  respectively represent the temperature-dependent kinetic rates of the hard degradable lignin fraction, easily degradable lignin fraction and condensed lignin. The numerical values of the kinetic rates and the initial hard and easily degradable fractions for the considered temperature range are given in [22] (Table 3).

The degradation and conversion of xylan and glucan follow the same pathway: polymers (xylan and glucan) are converted into their corresponding monomers (xylose and glucose) via intermediate oligosaccharides. Subsequently, the monomers are degraded to furfural, 5-hydroxymethylfurfural and other degradation products. Similar to the delignification process, it is assumed in [23] that both xylan and glucan in the solid consist of a fast-degrading fraction and a slow-degrading fraction. Considering first-order reactions, the conversion of xylan is described by

$$\begin{aligned}
 \frac{dXN_1}{dt} &= -k_{x1} \cdot XN_1 \\
 \frac{dXN_2}{dt} &= -k_{x2} \cdot XN_2 \\
 \frac{dXOS}{dt} &= k_{x1} \cdot XN_1 + k_{x2} \cdot XN_2 - k_{x3} \cdot XOS \\
 \frac{dX}{dt} &= k_{x3} \cdot XOS - (k_{x4} + k_{x5}) \cdot X \\
 \frac{dF}{dt} &= k_{x4} \cdot X - k_{x6} \cdot F
 \end{aligned}
 \tag{2}$$

while the conversion of glucan is given by

$$\begin{aligned}
 \frac{dGN_1}{dt} &= -(k_{g1} + k_{g6}) \cdot GN_1 \\
 \frac{dGN_2}{dt} &= -(k_{g2} + k_{g7}) \cdot GN_2 \\
 \frac{dGOS}{dt} &= k_{g1} \cdot GN_1 + k_{g2} \cdot GN_2 - (k_{g3} + k_{g8}) \cdot GOS \\
 \frac{dG}{dt} &= k_{g3} \cdot GOS - (k_{g4} + k_{g9}) \cdot G \\
 \frac{dHMF}{dt} &= k_{g4} \cdot G - k_{g5} \cdot HMF
 \end{aligned}
 \tag{3}$$

In (2),  $XN_1$  and  $XN_2$  denote respectively the fast- and slow-degrading xylan fractions,  $XOS$  denotes the xylo-oligosaccharides,  $X$  represents xylose and  $F$  represents furfural, while  $k_{xi}$  with  $i = 1 \dots 6$  are the temperature-dependent kinetic rates. Initial fractions of xylan in the solid as well as the parameters of the kinetic rates may be found in [23] (Tables 3 and 4). In (3),  $GN_1$  and  $GN_2$  denote respectively the fast- and slow-degrading glucan fractions,  $GOS$  denotes the gluco-oligosaccharides,  $G$  represents glucose and  $HMF$  represents 5-hydroxymethylfurfural, while  $k_{gj}$  with  $j = 1 \dots 9$  are the temperature-dependent kinetic rates. Initial fractions of glucan in the solid as well as the parameters of the kinetic rates may be found in [23] (Tables 5 and 6). Note that the states in (1) are expressed in percentages with respect to the original amount of lignin in the wood, which represents 22.36% of the dry wood mass (Table 1 in [22]), while the states in (2) and (3) are expressed in g per kg of dry wood.

### 3.2. Anaerobic Digestion

The anaerobic digestion model employed here is developed in [24]. It is an extension of the well-known ADM1 model [21], with the amendments made in [25], to accommodate the food waste digestion experimentally observed.

ADM1 is the most complex model describing the anaerobic digestion process. It includes the following conversion steps [21,26]: (i) disintegration of the composite material; (ii) hydrolysis of carbohydrates, proteins and lipids into their corresponding building blocks; (iii) acidogenesis, in which monosaccharides, amino-acids and long-chain fatty acids are fermented and short-chain organic acids, hydrogen, carbon dioxide and ammonia are produced; (iv) acetogenesis, in which various metabolic products of the previous degradation stages are mainly broken down into acetic acid, hydrogen and carbon dioxide, and (v) methanogenesis, in which mainly acetic acid and hydrogen are converted into methane. These conversion steps occur simultaneously and involve a variety of microorganisms. The process takes place in a continuous stirred tank reactor as schematically illustrated in Figure 5: waste is continuously supplied in the influent with the flow rate  $q$  ( $\text{m}^3/\text{day}$ ), and an equal flow is withdrawn from the reactor such that the liquid volume  $V_{liq}$  remains constant; the produced biogas (composed of methane, carbon dioxide and hydrogen) leaves the reactor with the flow rate  $q_{gas}$ .

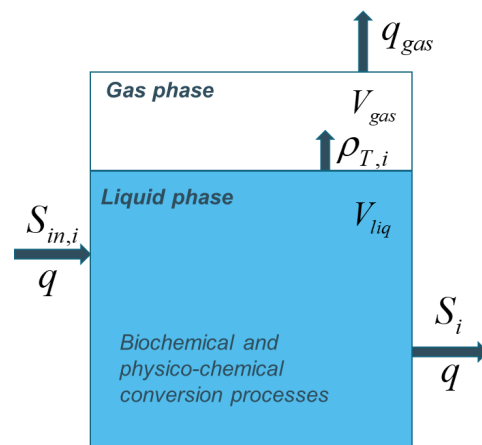


Figure 5. Anaerobic digestion system.

The ADM1 model consists of the mass balance of components in the solid-liquid and gas phases as summarised by

$$\frac{dS_i}{dt} = \frac{q}{V_{liq}}(S_{in,i} - S_i) + \sum_j \rho_j \nu_{ij} - \rho_{T,j} \quad (4)$$

$$\frac{dX_i}{dt} = \frac{q}{V_{liq}}(X_{in,i} - X_i) + \sum_j \rho_j \nu_{ij} \quad (5)$$

$$\frac{dS_{gas,i}}{dt} = -\frac{q_{gas}}{V_{gas}}S_{gas,i} + \frac{V_{liq}}{V_{gas}}\rho_{T,j} \quad (6)$$

where:  $S_i$  denotes the concentration of the soluble component  $i$ ,  $X_i$  denotes the concentration of the particulate component  $i$  and  $S_{gas,i}$  denotes the concentration in gas of either methane, carbon dioxide or hydrogen;  $S_{in,i}/X_{in,i}$  is the concentration in the influent of soluble/particulate component  $i$ ;  $\rho_j$  represents the reaction rate of process  $j$ , while  $\nu_{ij}$  represents the stoichiometric coefficient of component  $i$  on the process  $j$ ;  $\rho_{T,j}$  represents the transfer rate to the gas  $j$  and  $V_{gas}$  denotes the headspace volume. Note that the only soluble components which are transferred to the gas phase are methane, hydrogen and inorganic carbon. Except for nitrogen and carbon concentrations expressed in  $\text{kmol}/\text{m}^3$ , all the other concentrations are expressed as  $\text{kgCOD}/\text{m}^3$ .

In addition to the soluble matter, particulate matter and gas components, ADM1 includes balances for anions, cations and ion states, allowing for an accurate calculation of the process pH. The implementation reported by [25] consists of 35 differential equations and 8 algebraic equations, while the implementation [24] used in this work considers the acetate oxidation pathway, which is proved to make significant contributions to methane production and, in some cases, become more important than the acetoclastic methanogenesis. Compared to the original ADM1 implementation,

- two new processes are included, namely the acetate degradation by a new biomass group of acetate oxidisers and the decay of the new biomass group;
- hydrogen ions' concentration used to compute pH is a state of the model [27];
- some parameters are re-estimated to account for the digestion of waste with high nitrogen content such as food waste.

The main food waste characteristics and their translation into inlet concentrations of ADM1 model are also found in [24].

### 3.3. Ammonia Stripping

The ammonia stripping process [28–30] takes place in a closed vessel, where air is continuously sparged at its bottom and its content is continuously agitated. Ammonia is transferred from the liquid to the air bubbles, which leave the vessel. To facilitate the phase transition, the pH of the system must be increased, which requires the addition of a base. After the stripping, acid is added to re-establish the pH. The air outflow rich in ammonia is supplied to ammonia scrubbing process (not considered here), which allows the retrieval of ammonia as salt that can be used as fertiliser. A schematic representation of the ammonia stripping process is illustrated in Figure 6.

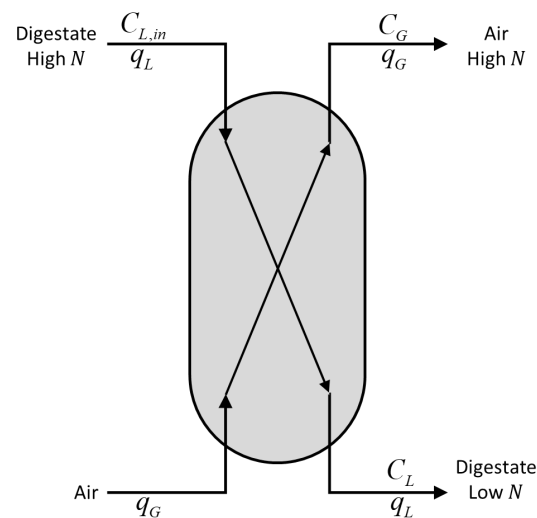


**Figure 6.** Schematic representation of the ammonia stripping process.

The mathematical model [28–30] describing the process relies on the mass balance for ammonia:

$$V_L \frac{dC_L}{dt} + \varepsilon_G V_L \frac{dC_G}{dt} = q_L(C_{L,in} - C_L) + q_G(C_{G,in} - C_G) \quad (7)$$

where  $q_G$  is the volumetric air flow rate ( $\text{m}^3/\text{s}$ ),  $C_{G,in}$  and  $C_G$  are the ammonia concentrations in the air entering and leaving the vessel ( $\text{kmol}/\text{m}^3$ ),  $V_L$  is the liquid volume ( $\text{m}^3$ ),  $C_{L,in}$  and  $C_L$  are the ammonia concentrations in the liquid phase entering and leaving the vessel ( $\text{kmol}/\text{m}^3$ ) and  $\varepsilon_G$  is the air holdup or the volume fraction of the air bubbles entrained in the liquid (dimensionless). Since [29]

- no ammonia is present in the influent air ( $C_{G,in} = 0$ );

- ammonia accumulation in the air bubbles is insignificant;
  - the equilibrium equation between air and liquid for any gas is given by Henry's law;
  - and the output stripping gas is probably not close to saturation,
- the mass balance (7) reduces to

$$V_L \frac{dC_L}{dt} = q_L(C_{L,in} - C_L) - q_G K_H C_L \quad (8)$$

where  $K_H$  denotes Henry's constant (dimensionless).

The efficiency of the ammonia stripping process is calculated as

$$\text{Removed ammonia(\%)} = \left(1 - \frac{C_L}{C_{L,in}}\right) \times 100 \quad (9)$$

### 3.4. Composting

Composting refers to the aerobic degradation of organic matter into valuable inert material (compost), which can be used as fertiliser for soil and plants.

The model of composting in biocells proposed in [31] relies on three main biochemical phenomena: (i) hydrolysis of the insoluble substrate, (ii) aerobic degradation of soluble substrate and (iii) biomass decay. The model describes the evolution of the main process variables (concentrations expressed in mol C/m<sup>3</sup>): soluble substrate  $S$ , representing the material that can be directly degraded; insoluble substrate  $I$ , representing the waste which needs to be hydrolysed before conversion; biomass concentration  $X$ ; liquid part  $L$ ; inert material (compost)  $M$ , and oxygen concentration  $O$ . As the biocell is a closed system, oxygen has to be supplied to maintain the biomass growth and the overall conversion.

The mass balance equations read:

$$\frac{dS}{dt} = -\frac{1}{Y_S} \mu(S, O) X + K_h I \quad (10)$$

$$\frac{dI}{dt} = -K_h I + \frac{1}{Y_I} b X \quad (11)$$

$$\frac{dX}{dt} = \mu(S, O) X - b X \quad (12)$$

$$\frac{dL}{dt} = \frac{1}{Y_L} \mu(S, O) X \quad (13)$$

$$\frac{dM}{dt} = -\left(1 - \frac{1}{Y_S} + \frac{1}{Y_L}\right) \mu(S, O) X + \left(1 - \frac{1}{Y_I}\right) b X \quad (14)$$

$$\frac{dO}{dt} = -\frac{1}{Y_O} \mu(S, O) X + FO_{in} \quad (15)$$

where

$$\mu(S, O) = \mu_{max} \frac{S}{K_S + S} \frac{O}{K_O + O} \quad (16)$$

describes the biomass growth, which is limited by the availability of soluble substrate and oxygen. The numerical values of the parameters [31] are given in Table 1.

**Table 1.** Parameters' values for the composting model [31].

Parameter	Value	Parameter	Value
$\mu_{max}$	0.72 h <sup>-1</sup>	$Y_S$	0.53
$K_S$	0.2573 mol/m <sup>3</sup>	$Y_I$	1.02
$K_O$	2.822 mol/m <sup>3</sup>	$Y_L$	1.34
$K_h$	18 × 10 <sup>-4</sup> h <sup>-1</sup>	$Y_O$	1.12
$b$	0.1368 h <sup>-1</sup>	$O_{in}$	8 mol/m <sup>3</sup>

### 3.5. Models' Integration and Scheduling

In a biorefinery, several processes are connected in a cascade, where the output of one process is fed as input to another process. Additionally, some processes may be operated in continuous mode, while others may be operated in batch or fed-batch mode. Hence, simulating the biorefinery operation and evaluating its efficiency requires models' integration and scheduling.

The biorefinery designed in this work consists of two branches, and its operation is indicated in Figure 7. The first branch comprises only one process, the steam refining process. Steam refining is a process which is operated in batch mode. Depending on the availability of wood waste and storage capacity, reactor size and considerations on energy use, the treatment of wood waste could be accomplished in real life in either one batch or repetitive batches. On the second branch, anaerobic digestion is a process operated in continuous mode, composting is a process operated in batch mode while ammonia stripping could be operated either continuously or in batch mode. For simplicity, we consider that the ammonia stripping process is operated in continuous mode, at the same rate as the anaerobic digestion process ( $q = q_L$ ). To buffer the transition between the continuous and batch operations, the low ammonia digestate exiting the ammonia stripping process is collected for a period of time  $\Delta t$  (days) in a tank, whose content is then transferred to a composting cell. Composting is a slow process which might not end in  $\Delta t$  days, the next period for filling in the buffer tank. Hence, several composting cells can be used in parallel, as shown in Figure 7.

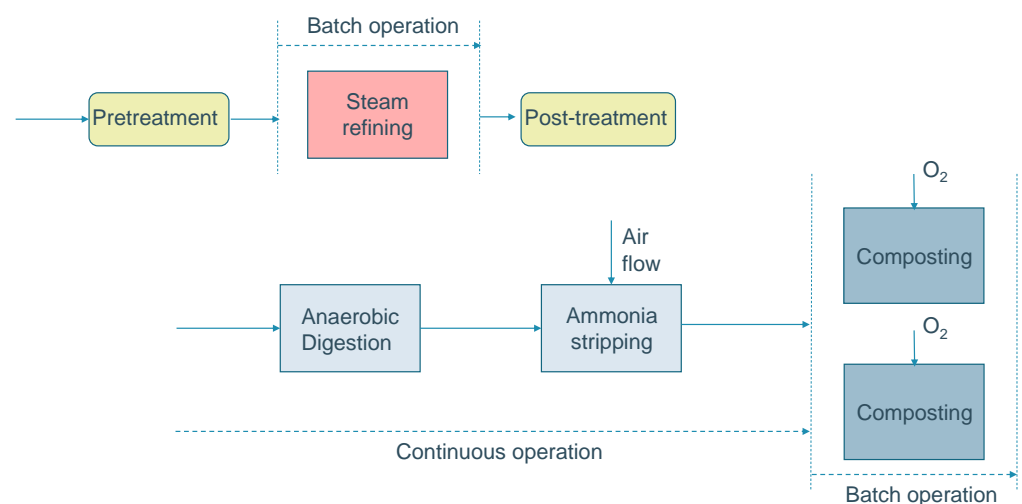


**Figure 7.** Biorefinery operation.

Assuming that no biochemical reaction takes place in the tank, its dynamics in terms of the states of the composting model are given by

$$\begin{aligned}
 \frac{dV}{dt} &= q \\
 \frac{dS}{dt} &= \frac{q}{V} \cdot (S_{in} - S) \\
 \frac{dI}{dt} &= \frac{q}{V} \cdot (I_{in} - I) \\
 \frac{dM}{dt} &= \frac{q}{V} \cdot (M_{in} - M)
 \end{aligned} \tag{17}$$

where  $V$  represents the volume of digestate accumulated in the tank,  $S$ ,  $I$  and  $M$  are respectively the concentrations of soluble, insoluble and inert matter in the tank, while  $S_{in}$ ,  $I_{in}$  and  $M_{in}$  are respectively the concentrations of soluble, insoluble and inert matter in the influent digestate.

Generally, the models employed to simulate a biorefinery are built for each specific process with the main goal of characterising its dynamics with a certain degree of detail. Thus, connecting two such models requires a good mapping of the first model's outputs to the second model's inputs. While anaerobic digestion is a complex process with a detailed characterisation of organic matter, its connection with the ammonia stripping model is straightforward, as the concentration of ammonia appears both in the effluent of the anaerobic digestion model and the influent of the ammonia stripping model ( $S_{NH_3} = C_{L,in}$ ). Assuming that no reaction takes place during ammonia stripping, the next step is to match the mix of digestate with wood to the states of the composting process.

In the first stage, the characteristics of digestate and the characteristics of wood are individually mapped to the states of the composting model. The conversion factors are respectively shown in Tables 2 and 3. Then, the initial states of the composting model are calculated as follows:

- Compute the volume of digestate collected from the anaerobic digestion process as  $V_{AD} = q \cdot \Delta t$ , where  $\Delta t$ (days) is the period of digestate collection and  $q$  ( $m^3$ /day) is the volumetric flow rate the anaerobic digester was operated with in the interval  $\Delta t$ . Note that  $V_{AD} = V$ , the volume in the tank at the time instant  $\tau = \Delta t$ ;
- Compute the volume of wood to be mixed with the digestate as  $V_w = w/\rho$ , where  $w$  (kg) is the mass of the wood and  $\rho$  ( $kg/m^3$ ) is its density;
- The concentrations of the soluble substrate, insoluble substrate and inert material entering the composting process are respectively given by

$$S_0 = \frac{x \cdot V_{AD} + 22.15 \cdot w}{V_{AD} + V_w} \quad (18)$$

$$I_0 = \frac{y \cdot V_{AD} + 12.75 \cdot w}{V_{AD} + V_w} \quad (19)$$

$$M_0 = \frac{z \cdot V_{AD}}{V_{AD} + V_w} \quad (20)$$

where  $x$ ,  $y$  and  $z$  (mol C/L) are respectively the concentrations of the soluble substrate, insoluble substrate and inert material in the tank at time instant  $\tau = \Delta t$ , i.e.,  $S(\tau)$ ,  $I(\tau)$  and  $M(\tau)$  given by (17). In (17),  $S_{in}(t)$ ,  $I_{in}(t)$  and  $M_{in}(t)$  are respectively the concentrations of the soluble substrate, insoluble substrate and inert material in the low-ammonia digestate entering the tank, which are calculated at each time instant using the conversion coefficients shown in Table 3. The coefficients in (18)–(20) (mol C/kg wood) are calculated based on data in Table 2.

**Table 2.** Conversion factors of wood characteristics into units of the composting model.

Component	Chemical Formula	Composting	g/(kg Wood) [22]	mol C/(kg Wood)
Rhamnose	$C_6H_{12}O_6$	S	1.00	0.0333
Galactose	$C_6H_{12}O_6$	S	6.70	0.223
Mannose	$C_6H_{12}O_6$	S	17.60	0.586
Xylose	$C_6H_{12}O_6$	S	209.30	6.97
Glucose	$C_6H_{12}O_6$	S	430.50	14.3
Klason lignin	$C_{81}H_{92}O_{28}$	I	177.00	9.47
Acid-soluble lignin	$C_{81}H_{92}O_{28}$	I	46.60	2.49
Acetyl group	COOH	I	35.40	0.786
Extractives	/	/	17.20	/
Others	/	/	58.70	/

**Table 3.** Conversion factors from anaerobic digestion to composting.

ADM1	State Composting	Conversion Factor mol C/kgCOD	Reference
$S_{su}$	S	31.3	[25]
$S_{aa}$	S	27.2	own calculation, [32]
$S_{fa}$	S	21.7	[25]
$S_{va}$	S	24.0	[25]
$S_{bu}$	S	25.0	[25]
$S_{pro}$	S	26.8	[25]
$S_{ac}$	S	30.0	[25]
$X_{ch}$	S	31.3	[25]
$X_{pr}$	S	27.2	own calculation, [32]
$X_{li}$	S	22.3	own calculation, [32]
$X_c$	I	25.2	own calculation, [32]
$X_{su}$	I	27.2	own calculation (C <sub>5</sub> H <sub>7</sub> O <sub>2</sub> N)
$X_{aa}$	I	27.2	own calculation (C <sub>5</sub> H <sub>7</sub> O <sub>2</sub> N)
$X_{fa}$	I	27.2	own calculation (C <sub>5</sub> H <sub>7</sub> O <sub>2</sub> N)
$X_{c4}$	I	27.2	own calculation (C <sub>5</sub> H <sub>7</sub> O <sub>2</sub> N)
$X_{pro}$	I	27.2	own calculation (C <sub>5</sub> H <sub>7</sub> O <sub>2</sub> N)
$X_{ac}$	I	27.2	own calculation (C <sub>5</sub> H <sub>7</sub> O <sub>2</sub> N)
$X_{h2}$	I	27.2	own calculation (C <sub>5</sub> H <sub>7</sub> O <sub>2</sub> N)
$X_{ac2}$	I	27.2	own calculation (C <sub>5</sub> H <sub>7</sub> O <sub>2</sub> N)
$X_I$	M	30	[25]

#### 4. Results and Discussion

The simulation results are based on the amounts and types of biowaste collected in the commune De Pinte in Flanders (Belgium). Via home-to-home collection, food waste is gathered every two weeks [18], while the wood waste is collected only once a year. Based on data given in Table 4, which shows the seasonality of the waste, a total amount of 395.508 tonnes of food waste is collected yearly. The yearly wood waste amount is 98.060 tonnes.

**Table 4.** Average amount of food waste collected per month in De Pinte [18].

Period	Collection Day	
	Day 1 [kg/month]	Day 2 [kg/month]
October–March	9557	18,340
April–September	15,260	22,773

As illustrated in Figures 3 and 7, the wood waste needs pretreatment before entering the steam refining process, while the reactor content needs posttreatment at the end of the process to retrieve the products of interest. No dynamic models are employed for these treatments but static blocks, which correct the amounts based on the experimental evidence. The pretreatment steps include washing, chipping, sieving and drying. It is assumed that after sieving, 95% of the wood chips has the proper size for steam refining, while the remaining 5% represents the wood residue which is processed via composting. Before entering the steam refining process, the small-sized wood chips need to be dried, the treatment in which the wood mass reduces by 10%. Consequently, the amount of

wood processed via steam refining (denoted as the main fraction of wood in Figure 3) is 83,841.3 kg, while the wood residue amount equals 4903 kg.

The steam refining conversion is influenced by the temperature and the length of the experiment. Figure 8 shows the evolution of the model states for a temperature  $T = 200\text{ }^{\circ}\text{C}$  and various experiment lengths. For the evaluation included below, an experiment length of 10 min is selected. This choice is motivated by the fact that no priority is given to any of the products of interest: lignin (solubilised lignin  $L_s$ ), fibres ( $L + XN + GN$ , where each component is the sum of the fast- and slow-degradable fractions) and oligosaccharides ( $XOS + GOS$ ). However, for longer experiments, the degradation of the products of interest occurs: the solubilised lignin degrades to condensed lignin, which is of no practical interest, while the oligosaccharides are converted into degradation products such as furfural ( $F$ ) and 5-hydroxymethylfurfural ( $HMF$ ).

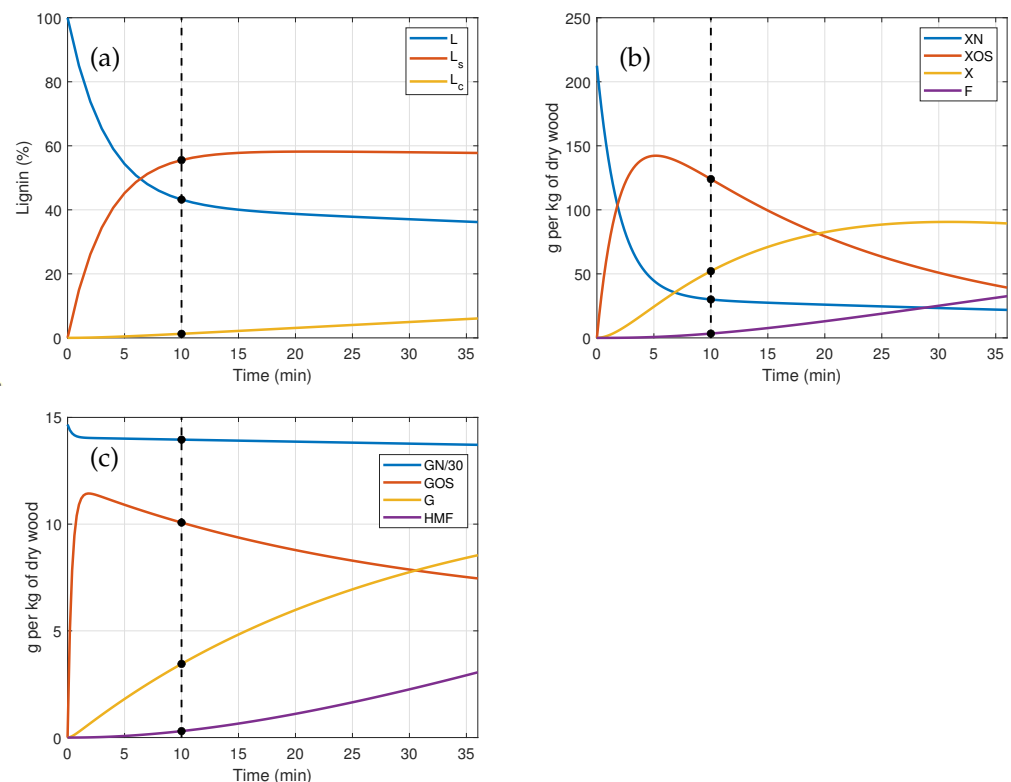


**Figure 8.** Steam refining: (a) Solubilised and solid-state lignin. (b) Xylan and its derivatives. (c) Glucan and its derivatives.

Figure 9 shows the conversion of the wood waste and the amounts of the products obtained, respectively, after steam refining (indicated in blue boxes) and after post-treatment (indicated in red boxes). These amounts are calculated based on the products' yields corresponding to a treatment duration of ten minutes and the amount of dry matter entering the process. The yields (see Figure 8) are as follows: 43.2% and 55.5% of original lignin content of wood, respectively, for the lignin remaining in the solid phase ( $L$ ) and the solubilised lignin ( $L_s$ ), 30 g/kg dry matter and 418.7 g/kg dry matter, respectively, for the xylan ( $XN$ ) and glucan ( $GN$ ), 124 g/kg dry matter and 10 g/kg dry matter, respectively, for xylo-oligosaccharides ( $XOS$ ) and gluco-oligosaccharides ( $GOS$ ). It is assumed that during postprocessing, 3% of fibres and 5% of oligosaccharides are lost. Note that the extract contains also monosaccharides (xylose and glucose) and can be used as a waste stream to feed another process or can be processed by anaerobic digestion.

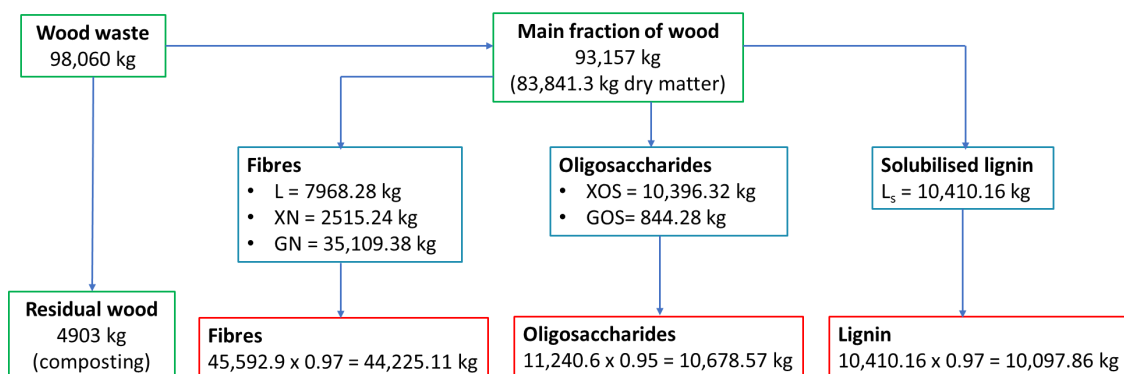


**Figure 9.** Products and their amounts obtained from wood steam refining: green boxes indicate feedstock, blue boxes show the products' amounts after steam refining treatment, and red boxes show the products' amounts after post-treatment.

The entire food waste collected throughout the year is processed by anaerobic digestion. Since this waste is available continuously, the simulation of the anaerobic digestion process is also performed for one year, with a constant supply of waste equal to 1083.6 kg/day. Similar to [24], it is assumed that the waste has the water mass, which implies that the digester is operated with a constant flow  $q = 1.0836 \text{ m}^3/\text{day}$ . Since low hydraulic retention times (defined as the ratio between the liquid volume and the feed flow rate) may lead to the reactor wash-out, in this simulation, the reactor liquid volume is selected as  $V_{liq} = 12 \text{ m}^3$  and the gas volume is chosen as  $V_{gas} = 3 \text{ m}^3$ . Figure 10 shows the obtained outflow rate of biogas, the outflow rate of methane, the volumetric production of methane and the composition of biogas for the entire operation span. The effluent of the digester is sent to the ammonia stripping process. The same liquid volume and the same feed flow rate as for the anaerobic digestion is assumed for this process. Air is continuously supplied such that efficiency of the removal in the range [80,90]% is achieved. Figure 11 illustrates the influent and effluent ammonia concentrations and the corresponding removed amounts.

The digestate with low ammonia content is collected for a period of 100 days in a storage tank. At the end of the collection period, the content of the storage tank is loaded in a biocell for composting, which receives a continuous air supply during the operation such that the oxygen is not limiting the growth of the aerobic microorganisms. Two biocells are used; the first one is loaded on days 100 and 300, the second biocell is loaded on days 200 and 400. The volume of digestate loaded in the composting cells on days 100, 200 and 300 amounts to  $108.36 \text{ m}^3$ , while the volume loaded on day 400 is  $71.46 \text{ m}^3$ , as it was collected only for 65 days. Figure 12 shows the evolution of the states of interest of the composting process taking place in each of the two employed biocells (one column corresponds to one cell). Note that the model predicts the content of compost expressed in  $\text{mol C}/\text{m}^3$ , while in the evaluation, one is interested in the amount of produced compost. For this, the conversion factor  $1 \text{ mol C compost} = 25.7 \text{ g compost}$  is used, which is determined based on the chemical formula assumed for compost ( $\text{C}_{204}\text{H}_{325}\text{O}_{85}\text{N}_{77}\text{S}$ ). The evaluation of the second branch of the proposed biorefinery is illustrated in Figure 13.

Overall, it may be concluded that the waste produced during one year in the commune De Pinte can be bioprocessed into 44,225.11 kg of fibres, 10,678.57 kg of oligosaccharides, 10,097.86 kg of lignin,  $113,730 \text{ m}^3$  of biogas, among which there is  $56,728 \text{ m}^3$  of methane, and 30,887.3 kg of compost. Additionally, nitrogen fertilizer could be produced from the removed ammonia. Although the obtained amounts are not obtained from an optimised operation, the proposed biorefinery design allows for the production of several high-value-added products.

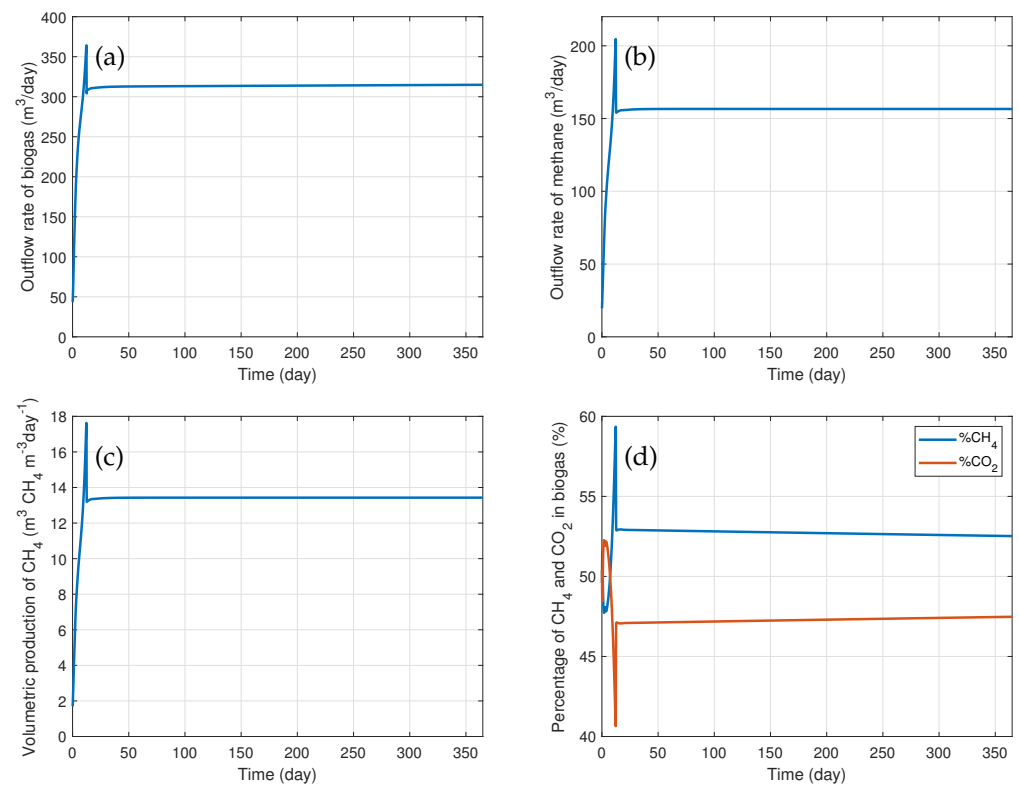


**Figure 10.** Anaerobic digestion: (a) Outflow rate of biogas. (b) Outflow rate of methane. (c) Volumetric production of methane. (d) Methane percentage in biogas.

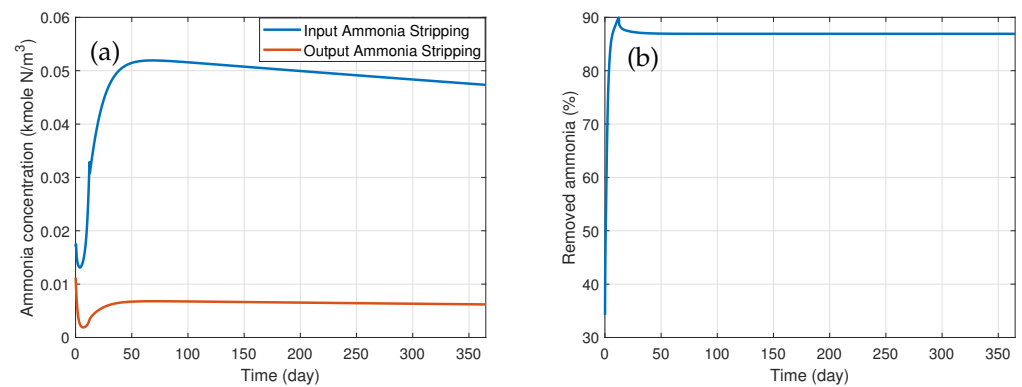


**Figure 11.** Ammonia stripping: (a) Influent and effluent ammonia concentrations. (b) Efficiency of the stripping process.

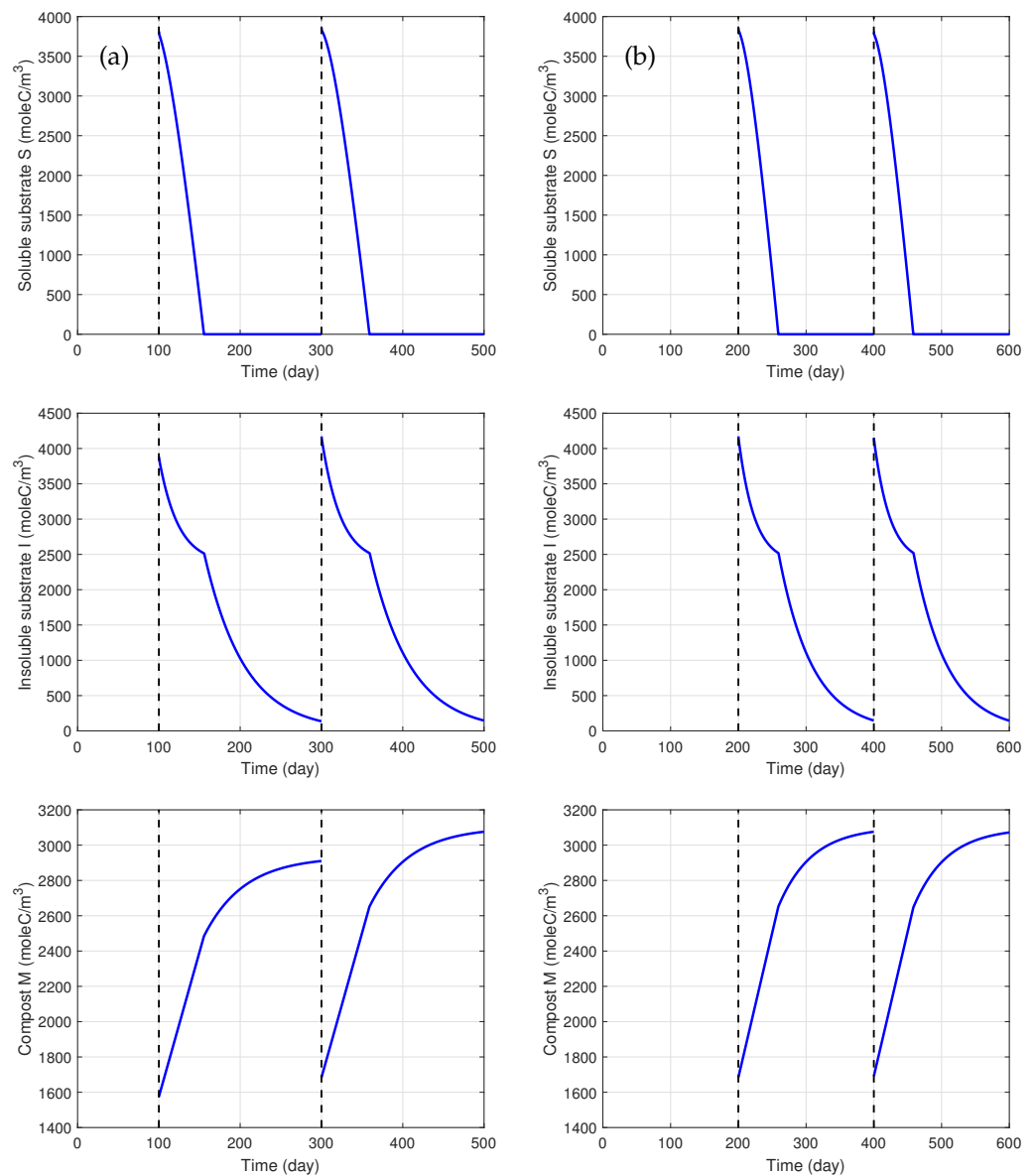


**Figure 12.** Composting process: Soluble substrate, insoluble substrate, inert material (compost) in (a) Cell 1 (left-hand-side column) and (b) Cell 2 (right-hand-side column).

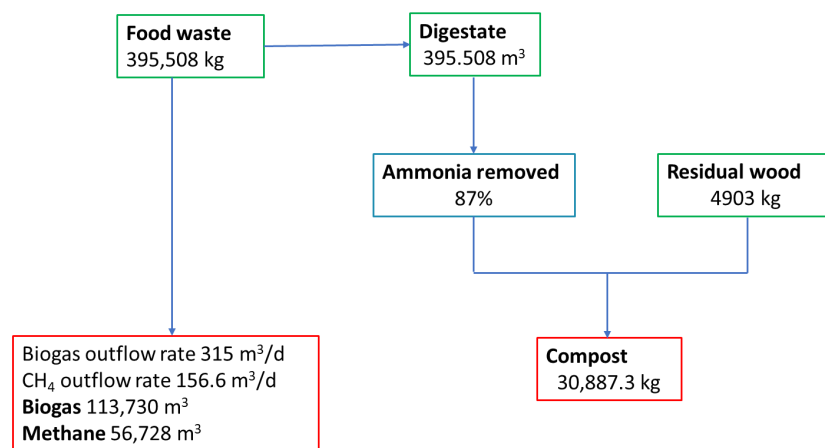


**Figure 13.** Products and their amounts obtained on the second branch of the biorefinery.

## 5. Conclusions and Perspectives

In this paper, the design of a small-scale biorefinery was presented and an evaluation based on data characterising the available biowaste on a yearly basis in a commune in Flanders was performed. The design started from the available feedstocks and was performed such that the side streams were minimised. The reported outcomes and the biorefinery operation represent a baseline scenario, which can be further improved through optimisation. The proposed biorefinery layout can be used for evaluation of feedstocks' potentials to produce high-valued products not only at the commune level but also at regional level. One of the main advantages of the proposed biorefinery is that it provides alternatives to the current practices at the local level, where food waste and landscaping waste are traditionally composted and burned.

The models employed in this biorefinery layout and the knowledge for their integration are the building blocks of the processing toolbox, which is one of the three core toolboxes in a decision support tool for the design of small-scale and flexi-feed biorefineries in a local setting. The processing toolbox will be linked with two additional toolboxes: (i) the bio-inventory toolbox [18] and (ii) the optimisation toolbox [33]. The former toolbox allows for drafting a survey of the locally available biowaste feedstocks and selecting one or multiple to be processed. Subsequently, this feedstock information will be employed by the processing toolbox to model and assess a suitable local and small-scale biorefinery layout, in a similar fashion as presented in this paper. To this end, the toolbox will be extended with new processes to account for the conversion of various feedstocks and the production of other high-value-added products [34,35]. Ultimately, as indicated above, the optimisation toolbox will employ the proposed biorefinery layout to further optimise the design and/or process settings. The decision support tool in its entirety will be detailed elsewhere.

**Author Contributions:** Conceptualization, M.S., V.D.B., S.A., S.B., M.P. and J.F.M.V.I.; software, M.S.; validation, M.S., V.D.B., S.A. and S.B.; writing—original draft preparation, M.S. and V.D.B.; writing—review and editing, M.S., V.D.B., S.A., S.B., M.P. and J.F.M.V.I.; supervision, J.F.M.V.I.; project administration, M.P. and J.F.M.V.I.; funding acquisition, S.A., M.P. and J.F.M.V.I. All authors have read and agreed to the published version of the manuscript.

**Funding:** This work was supported by the ERA-NET FACCE-SurPlus FLEXIBI Project, cofunded by VLAIO project HBC.2017.0176. V.D.B. is supported by FWO-SB Grant 1SC0922N. S.A. is supported by FWO grant 1224620N.

**Institutional Review Board Statement:** Not applicable.

**Informed Consent Statement:** Not applicable.

**Acknowledgments:** The authors would like to acknowledge the local council of De Pinte, Belgium, for their co-operation and the provision of the data necessary for this research.

**Conflicts of Interest:** The authors declare no conflict of interest. The funders had no role in the design of the study; in the collection, analyses or interpretation of data; in the writing of the manuscript, or in the decision to publish the results.

## References

1. Cherubini, F.; Jungmeier, G.; Wellisch, M.; Willke, T.; Skiadas, I.; Van Ree, R.; de Jong, E. Toward a common classification approach for biorefinery systems. *Biofuels Bioprod. Bioref.* **2009**, *3*, 534–546. [[CrossRef](#)]
2. Naik, S.N.; Goud, V.V.; Rout, P.K.; Dalai, A.K. Production of first and second generation biofuels: A comprehensive review. *Renew. Sustain. Energy Rev.* **2010**, *14*, 578–597. [[CrossRef](#)]
3. De Buck, V.; Polanska, M.; Van Impe, J. Modeling Biowaste Biorefineries: A Review. *Front. Sustain. Food Syst.* **2020**, *4*, 11. [[CrossRef](#)]
4. Mohr, A.; Raman, S. Lessons from first generation biofuels and implications for the sustainability appraisal of second generation biofuels. *Energy Policy* **2013**, *63*, 114–122. [[CrossRef](#)]
5. Leong, H.Y.; Chang, C.K.; Khoo, K.S.; Chew, K.W.; Chia, S.R.; Lim, J.W.; Chang, J.S.; Show, P.L. Waste biorefinery towards a sustainable circular bioeconomy: A solution to global issues. *Biotechnol. Biofuels* **2021**, *14*, 87. [[CrossRef](#)]
6. Bruins, M.E.; Sanders, J.P.M. Small-scale processing of biomass for biorefinery. *Biofuels Bioprod. Bioref.* **2012**, *6*, 135–145. [[CrossRef](#)]

7. Kolfshoten, R.C.; Bruins, M.E.; Sanders, J.P.M. Opportunities for small-scale biorefinery for production of sugar and ethanol in the Netherlands. *Biofuels Bioprod. Biorefin.* **2014**, *8*, 475–486. [[CrossRef](#)]
8. Jeevahan, J.; Anderson, A.; Sriram, V.; Durairaj, R.B.; Britto Joseph, G.; Mageshwaran, G. Waste into energy conversion technologies and conversion of food wastes into the potential products: A review. *Int. J. Ambient. Energy* **2021**, *42*, 1083–1101. [[CrossRef](#)]
9. Isikgor, F.; Becer, C. Lignocellulosic Biomass: A Sustainable Platform for Production of Bio-Based Chemicals and Polymers. *Polym. Chem.* **2015**, *6*, 4497–4559. [[CrossRef](#)]
10. Clark, J.H.; Deswarte, F.E.I. The Biorefinery Concept—An Integrated Approach. In *Introduction to Chemicals from Biomass*; Clark, J.H., Deswarte, F.E.I., Eds.; John Wiley & Sons, Ltd.: Chichester, UK, 2014; pp. 1–20. [[CrossRef](#)]
11. Sukumara, S.; Faulkner, W.; Amundson, J.; Badurdeen, F.; Seay, J. A multidisciplinary decision support tool for evaluating multiple biorefinery conversion technologies and supply chain performance. *Clean Technol. Environ. Policy* **2014**, *16*, 1027–1044. [[CrossRef](#)]
12. Martinkus, N.; Latta, G.; Rijkhoff, S.A.M.; Mueller, D.; Hoard, S.; Sasatani, D.; Pierobon, F.; Wolcott, M. A multi-criteria decision support tool for biorefinery siting: Using economic, environmental, and social metrics for a refined siting analysis. *Biomass Bioenergy* **2019**, *128*, 105330. [[CrossRef](#)]
13. Petre, E.; Selişteanu, D.; Roman, M. Control schemes for a complex biorefinery plant for bioenergy and biobased products. *Bioresour. Technol.* **2020**, *295*, 122245. [[CrossRef](#)] [[PubMed](#)]
14. Prunescu, R.M.; Blanke, M.; Jakobsen, J.G.; Sin, G. Model-based plantwide optimization of large scale lignocellulosic bioethanol plants. *Biochem. Eng. J.* **2017**, *124*, 13–25. [[CrossRef](#)]
15. Cheali, P.; Gernaey, K.V.; Sin, G. Synthesis and design of optimal biorefinery using an expanded network with thermochemical and biochemical biomass conversion platforms. *Comput. Aided Chem. Eng.* **2013**, *32*, 985–990. [[CrossRef](#)]
16. Cheali, P.; Quaglia, A.; Gernaey, K.V.; Sin, G. Effect of Market Price Uncertainties on the Design of Optimal Biorefinery Systems—A Systematic Approach. *Ind. Eng. Chem. Res.* **2014**, *53*, 6021–6032. [[CrossRef](#)]
17. Zondervan, E.; Nawaz, M.; de Haan, A.B.; Woodley, J.M.; Gani, R. Optimal design of a multi-product biorefinery system. *Comput. Chem. Eng.* **2011**, *35*, 1752–1766. [[CrossRef](#)]
18. De Buck, V.; Sbarciog, M.; Polanska, M.; Van Impe, J. Assessing the local biowaste potential of rural and developed areas using GIS-data and clustering techniques: Towards a decision support tool. *Front. Chem. Eng.* **2022**, *4*, 825045. [[CrossRef](#)]
19. European Biogas Association. *Annual Report 2020*; European Biogas Association: Brussels, Belgium, 2021. Available online: <https://www.europeanbiogas.eu/eba-gie-biomethane-map/> (accessed on 31 March 2022).
20. Sbarciog, M.; Bhonsale, S.; De Buck, V.; Akkermans, S.; Polanska, M.; Van Impe, J. Modelling and simulation of co-digestion in anaerobic digestion systems. In Proceedings of the 10th Vienna International Conference on Mathematical Modelling (MATHMOD 2022), Vienna, Austria, 27–29 July 2022.
21. Batstone, D.J.; Keller, J.; Angelidaki, I.; Kalyuzhnyi, S.V.; Pavlostathis, S.G.; Rozzi, A.; Sanders, W.T.M.; Siegrist, H.; Vavilin, V.A. Anaerobic Digestion Model No. 1. In *IWA STR No. 13*; IWA Publishing: London, UK, 2002.
22. Borrega, M.; Nieminen, K.; Sixta, H. Effects of hot water extraction in a batch reactor on the delignification of birch wood. *BioResources* **2011**, *6*, 1890–1903.
23. Borrega, M.; Nieminen, K.; Sixta, H. Degradation kinetics of the main carbohydrates in birch wood during hot water extraction in a batch reactor at elevated temperatures. *Bioresour. Technol.* **2011**, *102*, 10724–10732. [[CrossRef](#)]
24. Nguyen, H.H. Modelling of Food Waste Digestion Using ADM1 Integrated with Aspen Plus. Ph.D. Thesis, University of Southampton, Southampton, UK, 2014.
25. Rosen, C.; Jeppsson, U. *Aspects on ADM1 Implementation within the BSM2 Framework*; Department of Industrial Electrical Engineering and Automation, Lund University: Lund, Sweden, 2006.
26. Weinrich, S.; Nelles, M. *Basics of Anaerobic Digestion—Biochemical Conversion and Process Modelling*; DBFZ: Leipzig, Germany, 2021.
27. Thamsirirot, T.; Murphy, J. Modelling mono-digestion of grass silage in a 2-stage CSTR anaerobic digester using ADM1. *Bioresour. Technol.* **2011**, *102*, 948–959. [[CrossRef](#)]
28. Degermenci, N.; Nuri Ata, O.; Yıldız, E. Ammonia removal by air stripping in a semi-batch jet loop reactor. *J. Ind. Eng. Chem.* **2012**, *18*, 399–404. [[CrossRef](#)]
29. Degermenci, N.; Yıldız, E. Ammonia stripping using a continuous flow jet loop reactor: Mass transfer of ammonia and effect on stripping performance of influent ammonia concentration, hydraulic retention time, temperature, and air flow rate. *Environ. Sci. Pollut. Res.* **2021**, *28*, 31462–31469. [[CrossRef](#)] [[PubMed](#)]
30. Kofi, A.-W.; Martino, C.J.; Wilmarth, W.R.; Bennett, W.M.; Peters, R.S. Modeling air stripping of ammonia in an agitated vessel. In *Office of Scientific & Technical Information Technical Reports*; University of North Texas Libraries, UNT Digital Library: Aiken, SC, USA, 2005. Available online: <https://digital.library.unt.edu/ark:/67531/metadc873356/m1/6/> (accessed on 20 July 2021).
31. Martalo, G.; Bianchi, C.; Buonomo, B.; Chiappini, M.; Vespri, V. Mathematical modeling of oxygen control in biocell composting plants. *Math. Comput. Simul.* **2020**, *177*, 105–119. [[CrossRef](#)]
32. Lopez, V.M.; De la Cruz, F.B.; Barlaz, M.A. Chemical composition and methane potential of commercial food wastes. *Waste Manag.* **2016**, *56*, 477–490. [[CrossRef](#)] [[PubMed](#)]
33. De Buck, V.; Nimmegeers, P.; Hashem, I.; Muñoz López, C.A.; Van Impe, J. Exploiting Trade-Off Criteria to Improve the Efficiency of Genetic Multi-Objective Optimisation Algorithms. *Front. Chem. Eng.* **2021**, *3*, 582123. [[CrossRef](#)]

- 
34. Wagemann, K.; Tippkotter, N. (Eds.) *Biorefineries*; Springer: Cham, Switzerland, 2019.
  35. Mohan, S.V.; Varjani, S.; Pandey, A. (Eds.) *Microbial Electrochemical Technology*; Elsevier: Amsterdam, The Netherlands, 2018.